

Engineering Proprioceptive Implants via Surgical and Regenerative Approaches: Preliminary Interpretations

SIDDHARTHA DAS¹

¹*Department of Chemical Engineering, IIT Bombay, Mumbai, 400076, India*

H.D. SARMA^{2*}

²*Radiation Biology and Health Sciences Division, BARC, Mumbai, 400085, India*

AND

JAYESH BELLARE^{1,3*}

¹*Department of Chemical Engineering and* ³*Wadhvani Research Centre for Bioengineering, IIT Bombay, Mumbai, 400076, India*

*Corresponding authors: hdsarma@barc.gov.in, jb@iitb.ac.in

The periodontal ligaments are a group of specialized connective tissue fibres with vascular and neural elements that essentially attach a tooth to the alveolar bone. Endosseous dental implant replacing a lost tooth, gets ankylosed to the alveolar bone without intervening periodontal fibres (osseointegration). Hence, proprioception, one of the most important function of periodontal ligament is not elicited by commercial dental implants currently in use. To salvage the flaw, in our proof-of-principle trial in rabbits, biodegradable nanofibres were coiled around the additive manufactured (AM) customized titanium implants. Further, human dental pulp stem cells (DPSCs), adult mesenchymal stem cells of neuro-ectodermal origin, were seeded on the nanofibrous coated, orthotopically placed 3D-printed titanium implants and were induced to differentiate into neural cell lineages. The invivo anchoring mechanism of these biodegradable neuro-supportive scaffold coated implants could probably be “proprioceptive osseointegration” instead of defaults events leading to normal “osseointegration” and could exhibit features similar to periodontium, having possible anastomosis between the severed nerve terminals present in the wall of the extraction socket relaying to/from brain and newly differentiated neural cells present in the regenerated neo-tissue complex, gradually replacing the biodegradable scaffold and may eventually results in the development of proprioceptive osseointegrated root-form endosseous dental implants in near future.

Keywords: Proprioception; Experimental Surgery; Titanium Dental Implant; 3D Printing; Stem Cells

1 Introduction

2 Co-ordinated and precise oral-motor movements depend on afferent inputs from specialized sensory
3 organs in the orofacial region. Among others, a healthy natural tooth consists of extremely
4 sensitive mechanoreceptors located in the periodontal ligament (PDL)¹ cushioning its root(s). These
5 components largely serve in motor behaviour of maxillo-mandibular complex involving functions such
6 as mastications, biting etc. Earlier studies have established the rich sensory innervation of periodontal
7 ligament via the trigeminal pathways through superior or inferior alveolar branches.² The nerve fibre
8 enters the PDL in the apical region and perforating the lateral wall of the alveolus, give rise to the
9 plexus of nerves. The single myelinated nerve fibres originate from the main nerve bundle lose their
10 myelin sheath and further terminates in free nerve endings, Ruffini like mechanoreceptors, Meissner

11 corpuscles and spindle like pressure/vibration endings.³ Activity of these sensory receptors relies on
12 stimulus applied on teeth and supporting structures and transmits afferent information to the central
13 nervous system.¹

14 In cases of edentulism, prosthodontic treatment considerations such as dental implants are favoured
15 and advocated.⁵ Although oral implant enjoys a high success rate and is secured in bone through a
16 process called osseointegration,^{6,7} the exclusion of PDL and its functionality such as proprioception
17 after the healing events render the conventional osseointegrated implant rather a compromised
18 prosthetic substitute.⁸ Of note, years of research studies lead to the evidence of probability to a
19 widespread and admitted concept of interruption of neural circuitry in osseointegrated dental implants,
20 following absence of the periodontal mechanoreceptors in the juxtaposed tissue, effectuating failure in
21 the propagation of primary sensory inputs.^{2,9-12} Hence, to address the pitfall, numerous contemporary
22 attempts towards the engineering of PDL tissues, interfacing alveolar bone or endosseous implants have
23 been reported globally.¹³⁻²³

24 The innervation of the aforementioned PDL via the trigeminal nerve for proprioception in humans
25 has been studied extensively.²⁴ Briefly, the peripheral part of the trigeminal nerve consists of CN V1
26 (ophthalmic div.), CN V2 (maxillary div.) and CN V3 (mandibular div.). The purely sensory, CN
27 V2 (maxillary nerve), emerges between the ophthalmic and mandibular nerves, courses and divides
28 into anterior and middle superior alveolar branches further continuing in the anterior and lateral
29 wall of maxillary sinus to innervate anteriors and premolar teeth respectively. Additionally, posterior
30 superior alveolar nerves also arises from CN V2 in the pterygopalatine fossa and continues through the
31 infratemporal surface of the maxilla and subsequently innervates second and third molars, the roots of
32 the maxillary first molar, buccal mucosa and posterior maxillary gingivae.²⁵ The CN V3 (mandibular
33 div.), a mixed cranial nerve continues from the lateral part of trigeminal ganglion and is composed of
34 large sensory and small motor root. The sensory root innervates the mandibular teeth and gums, auricle,
35 external acoustic meatus, skin of temporal region, tympanic membrane etc.²⁶ while the motor branch
36 innervates the muscles of 1st pharyngeal arch.²⁷ The peripheral sensory branches from CN V1, CN
37 V2 and CN V3 gradually merge at the trigeminal ganglion (Gasserian ganglion/semilunar ganglion)
38 located in the depression on the petrous apex of temporal bone known as Meckel's cave.²⁸ Dorsal to the
39 trigeminal ganglion and ventral to the pons, trigeminal root consisting of large sensory and small motor
40 division, leaving the pons at the root exit zone could be noted. The sensory root consisting of central
41 processes of pseudo-unipolar neurons in the trigeminal ganglion, extends into pons and communicates
42 with nuclei in the brainstem. The sensory nucleus extends from the midbrain superiorly to upper cervical
43 spinal cord and consists of mesencephalic, principal and the spinal trigeminal nuclei. On the other
44 hand, the trigeminal motor nucleus is located in the mid-pons, medial to the principal sensory nucleus
45 and could be traced back to its union with CN V3.²⁹

46 The forenamed mesencephalic nucleus, a slender columnar structure, extends in the dorsomedial
47 tegmentum from the level of the trigeminal motor nucleus in the pons to the rostral midbrain³⁰ is
48 rather unique for containing cell bodies of primary sensory neurons conveying information from
49 proprioceptors present in oculomotor/masticatory system^{31,32} and are involved in a wide range of
50 activities such as pressure sensation from teeth, palate, TMJ capsule, etc.³³

51 The principal sensory nucleus receives general somatic afferent fibres and consists of ventrolateral
52 and dorsomedial nuclei. CN V1, CN V2, and CN V3 supplies information to the ventrolateral nucleus
53 while primary afferent inputs from the oral cavity transduce information to the dorsomedial nucleus.³⁴
54 The extension of spinal nucleus of trigeminal nerve is caudally to the outer lamina of the dorsal horn of
55 the upper three to four cervical spinal segments and contains three different subnuclei in a rostrocaudal
56 direction: the subnucleus oralis, the subnucleus interpolaris, and the subnucleus caudalis.³⁴ Subnucleus

57 oralis receives afferent inputs from nasal and oral regions,³⁵ subnucleus interpolaris and subnucleus
58 caudalis receives information from the cutaneous portions of the face however the latter receives
59 extensive sensory inputs from the cheek, jaw, and forehead.³⁴ Medial to the principal sensory nucleus
60 in the mid-pons lies the motor nucleus and conveys special visceral efferent fibers.³⁶ The fibres of the
61 motor nucleus is closely associated with mesencephalic nucleus and in cooperation regulates the bite
62 force.^{36,37}

63 The fibres ascends via various tracts and/or lemniscus for their respective projection in the thalamus
64 [venteroposterior (VP) nucleus], continues through the posterior limb of the internal capsule and
65 eventually allowing the oro-facial area to be represented in the postcentral gyrus, the sensory cortex, or
66 Brodmann areas 3, 1, and 2.^{36,38}

67 In view of the above discussed trigeminal system and its central connections for oral proprioceptive
68 function in humans, we hypothesized that our modifications of coating systems^{39–41} such as neuro-
69 supportive nanofibrous coating with exogenous mesenchymal stem cells⁴² in endosseous dental
70 implants can generate proprioceptive features. We, therefore, decided to investigate the proof-
71 of-principle mechanism in rabbit study models because its trigeminal system⁴³ and somatotopic
72 organization⁴⁴ shares similar homology to that in humans.^{45–47} Hence, the customized endosseous
73 titanium dental implants were conceptualized, designed, and later fabricated by additive manufacturing
74 (AM)/manually and were further subjected to post-fabrication electrospun neuro-supportive nanofibrous
75 coating in conjunction with exogenous mesenchymal stem cells for orthotopic implantation in rabbits
76 to reinstate proprioceptive functions.

77 **Methods**

78 *0.1. Procurement Of Animals*

79 The proof-of-concept animal trials were conducted at Experimental Facility & Radioisotope Laboratory,
80 Radiation Biology and Health Sciences Division (RBHSD), Bhabha Atomic Research Centre (BARC),
81 Mumbai, under the Department of Atomic Energy, Government of India. The research protocol was
82 reviewed and approved by the panel of the ethics committee for laboratory animal research of BARC,
83 RBHSD, Mumbai, BARC-IITB (Animal study proposal no. BAEC /14/2019), and was performed
84 in accordance with the guidelines of the Committee for the Purpose of Control and Supervision of
85 Experiments on Animals (CPCSEA), Ministry of Social Justice and Empowerment, Government of
86 India. In addition, all experimental surgical protocols and procedures as well as the post-operative care
87 and monitoring were supervised by the senior scientific officer and respective staff of RBHSD, BARC,
88 Mumbai. The methodology for the present study is as per International Standard ISO-10993-677.⁴⁸

89 Three healthy adult male New Zealand white rabbits were used in the study (Supplementary
90 Tables). The pathogen free rabbits were obtained from Reliance Life Sciences Pvt. Limited, Mumbai,
91 India, after due approval from the IAEC. Each rabbit was numbered and was kept in cages under
92 standardized conditions.⁴⁹ The animals were kept on a 12-hour day/night cycle with *ad libitum* access
93 to food and water.

94 *0.2. Radiographic Planning & Measurements*

95 Series of approximate dental measurements were considered in rabbits with Planmeca ProMax® 3D
96 Mid imaging unit (Planmeca, Helsinki, Finland) and saved as DICOM files and were later analysed
97 with dedicated softwares (OsiriX® 8.5, Osirix Foundation, Geneva, Switzerland, <https://www.osirix-viewer.com> and Planmeca Romexis version 4.6.0, Planmeca, Finland). Mesiodistal width, buccolingual

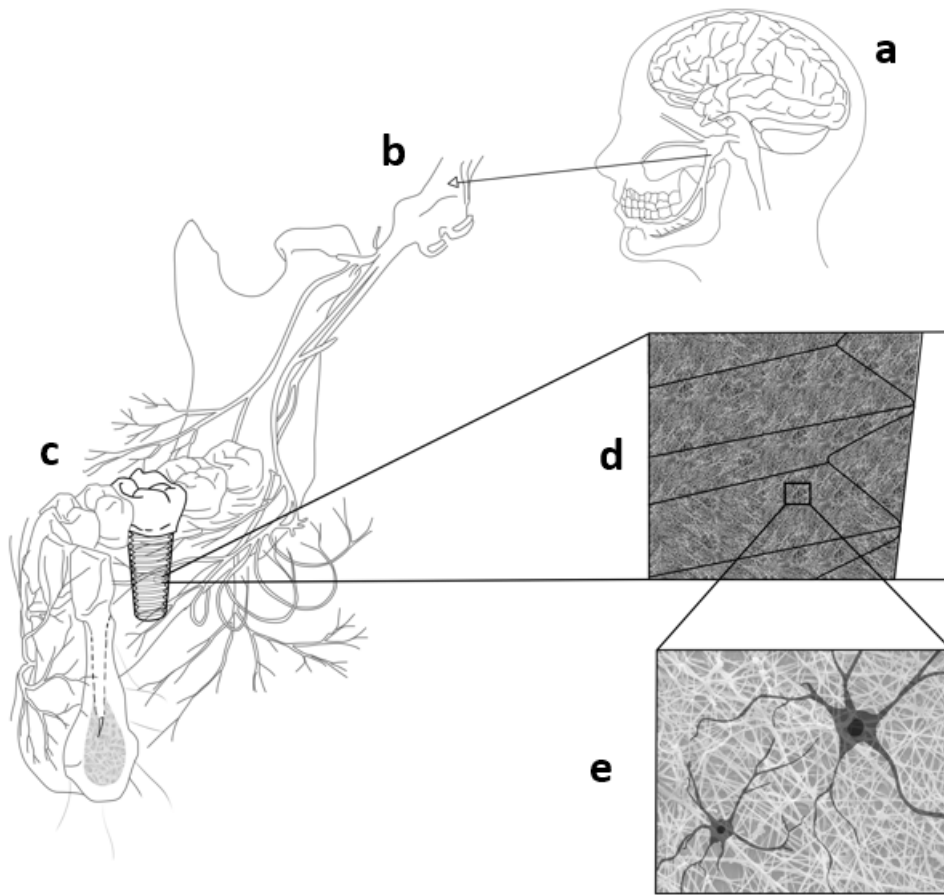


FIG. 1. Probable mechanism for the development of proprioception in the modified root-form endosseous dental implant: Here, a portion of the mandible with its neural innervation is depicted for understanding the significance. a - Human brain with trigeminal ganglion and its branches - ophthalmic (V1), maxillary (V2), and mandibular (V3) branches. b - The posterior division of the mandibular nerve gives off sensory branches viz. lingual, long buccal and inferior alveolar nerves. c - Portion of the mandible with anterior and posterior teeth and modified dental implant replacing a posterior teeth, d - Magnified image of a portion of modified dental implant coated with electrospun nanofibres, seeded with exogenous dental pulp mesenchymal stem cells, e- Fraction of mesenchymal stem cells in the nanofibrous coating are differentiated to neural cells upon receiving appropriate signals. These differentiated neural cells present in the regenerated neo-tissue complex may anastomose with the severed/terminal sensory branches of alveolar division originating from trigeminal nerve supplying the wall of the alveolar socket during the healing phase and thereby completing the neural circuitry, resulting in the development of proprioceptive sensation in those implants.

99 width, mid-point of incisal margin to apex length, a crude estimate of the curvature in mandibular
100 left central incisor and pre-implantation evaluation of jaw anatomy were thoroughly investigated by an
101 experienced bioengineer and surgeon (Supplementary Fig). The range of dimensional values obtained
102 specifying the tooth of interest i.e., mandibular left central incisor, (301, modified Triadan system⁵⁰⁻⁵¹)
103 was utilized for fabricating the implants.

104 0.3. *Implant Fabrications*

105 Seven titanium dental implants were shaped and fabricated manually from intramedullary titanium
106 elastic nail (1×4 mm) (Uma Surgicals, Mumbai, India) in the workshop of MOD Lab, Design
107 and Inspection Section (EmA&ID), BARC, Mumbai, by an experienced bioengineer and surgeon.
108 The macro design features with trapezoidal cross-section ($n = 7$, diameter = 3.65 ± 0.081 mm,
109 best conformed/suited, $n = 1$ is installed) for the tooth of interest were in compliance with the
110 precise information acquired through CBCT imaging of the craniofacial region in rabbit study models
111 (Supplementary Fig). Likewise, 3D printed customized rabbit dental implants ($n = 7$, diameter =
112 3.65 ± 0.081 mm, best conformed/suited, $n = 1$ is installed) were designed using the 3D design
113 software, Solidworks 2018 (Dassault Systemes Solidworks Corporation, Waltham, MA, USA) and
114 exported as .STL files by an experienced bioengineer and surgeon (Supplementary Fig). A DMLS
115 additive manufacturing system (EOS M280, EOS GmbH, Krailling, Germany) was used to print the
116 biocompatible titanium (6%)- aluminium-(4%) vanadium extra low interstitial (ELI) grade 23 powder
117 with particle size distribution of 5 - 55 μm . A ytterbium laser system was utilized for layer by layer
118 fabrication of implants with 33 W laser power, 1000 mm/s laser speed and a wavelength of 1060-1100
119 nm, with layer size of 60 μm (Supplementary Fig). Post-production cleaning steps were followed as
120 described previously.⁵²

121 0.4. *Stem Cell Culture*

122 Human Dental Pulp Stem Cells were obtained as described previously⁴² and were maintained in low
123 glucose MEM-alpha (Gibco, Invitrogen, Carlsbad, CA, USA), supplemented with 18% fetal bovine
124 serum (MSC-FBS, Gibco) and 100 g/ml streptomycin (Invitrogen/Gibco, Grand Island, NY; US), 100
125 U/ml penicillin (Invitrogen/Gibco), 0.1 mM ascorbic acid (Sigma-Aldrich Corporation, St. Louis, MO,
126 US), and 2 mM L-glutamine (Gibco). Cells were maintained at 37 °C in a humidified atmosphere of
127 5% CO₂.

128 0.5. *Coating Of Titanium Implants*

129 The fabricated implants (manually prepared and 3D printed implants) of size 3.65 ± 0.081 mm diameter
130 $\times 27 \pm 0.81$ mm length were coated with neuro-supportive nanofibres composed of a composite
131 blend of polycaprolactone (Mw-80,000) 8.33 (w/v) % (Sigma Aldrich, USA), gelatine type A 0.833
132 w/v % (Sigma Aldrich, USA), in 2,2,2-Trifluoroethanol (Sigma Aldrich, USA).⁴² Uncoated titanium
133 rabbit dental implant was used as controls (Supplementary Fig). The technology for fabrication of
134 neuro-supportive nanofibrous coating on the surface of titanium implants by modified electrospinning
135 technique has been described previously by the same author⁴² and was performed by carefully placing
136 the fabricated dental implant (attached to the rotating shaft of DC motor) in between the syringe tip and
137 collector plate⁴² in the *Silicate Lab of J.B., Chemical Engineering, IIT Bombay* (Supplementary Fig).
138 The modification of the electrospinning apparatus for fabricating nanofibrous coating, its subsequent
139 physico-chemical characterization, and in vivo response have been described exhaustively in our earlier
140 and related study.³⁹⁻⁴⁰ The thickness of the elastomeric porous neuro-supportive nanofibrous coating on
141 the surface of dental implants was chosen carefully to permit proper insertion (i.e. just enough loose to
142 allow inward movement in the fresh extraction socket) and adequate intimate contact of nanofibrous
143 coating with the inner wall of fresh extraction socket for ensuring necessary primary stability for
144 uneventful healing, post-surgery. Prior to surgery, the uncoated and neuro-supportive nanofibrous coated
145 implants were sterilized by irradiating with 25 KGy of gamma exposure in a gamma chamber (GC-900,

146 BRIT India make), Food Technology Division, BARC, Mumbai, India. Samples for gamma irradiation
147 were delivered in sealed and sterile containers.

148 0.6. *Stem Cells & Coating*

149 The Human Dental Pulp Stem Cells (hDPSCs) were trypsinized after reaching a state of 80% confluency
150 (3×10^6 cells/flask/vial) and were suspended and agitated gently in vials ($n = 2$) with 2 ml complete
151 media to generate a homogeneous solution. Sterile insulin syringes (BD 1-mL conventional insulin
152 syringes) was used to insert homogenous cell suspension inside the layers of nanofibrous coating by
153 an experienced bioengineer and surgeon. Additionally, the cell suspension (vial/implant) was pipetted
154 carefully on the sterile surface of the nanofibrous coated implants whilst applying gradual rotational
155 motion along its transverse axis. The nanofibrous coated implants with stem cells were incubated for 15
156 mins and were transferred into a 24 well cell culture plate and further incubated in complete medium
157 under conditions of 37°C, 98% humidity and 5% CO₂ for 24 hours. All cell culture procedures were
158 accomplished in a laminar flow hood, adhering to the sterility protocols of the materials and solutions.

159 0.7. *Surgical Instruments & Adjunctives*

160 Basic oral surgical instruments like pediatric extraction forceps, oral surgical kit, dental explorers,
161 Metzenbaum scissors, towel clamps were obtained from GDC instruments, India. Hemostats, tissue
162 pliers were purchased from Hu-Friedy, Chicago, IL, USA. Mallet hammer, Hohman's bone spike, bone
163 spike A.O type, Farabeuf periosteum elevator were acquired from Uma Surgicals, Mumbai, India.
164 PeroxiDam, a light-curing material was purchased from Latus, Ukraine. Additionally, flexible blades
165 were fabricated by flattening the syringe needles (3/8 inch - 3 1/2 inches, BD Precision Glide™ needles)
166 in the workshop of MOD Lab, BARC, Mumbai for severing Sharpey's fibers within the periodontal
167 ligament. The blades were sharpened in the grinding motor by an extremely delicate touch for obtaining
168 sharp contour at the edges⁵³ by an experienced bioengineer and surgeon. All surgical instruments and
169 accessories were autoclaved following standard protocols.⁵⁴

170 0.8. *Experimental Surgical Protocol For Customized Dental Implants Placed In Mandible Of Rabbits*

171 For clinical chemistry, hemogram and other relevant determinants, the sampling of blood (~3 ml) from
172 rabbits were performed prior to the day of surgery (Supplementary Tables). Pre-operative assessment
173 (extraoral and intraoral) along with administration of Enrofloxacin (Bayrocin, Bayer) intramuscularly
174 (5 mg kg^{-1} q.d., was continued for 3 days. On the day of surgery, induction of surgical anaesthesia
175 was achieved in rabbits with intramuscular injection of 35 mg kg^{-1} body weight of ketamine and 5
176 mg kg^{-1} body weight of xylazine (Indian Immunologicals). The intraoral region was cleaned prior to
177 surgery with antiseptic 2% chlorhexidine gluconate and 2% povidone-iodine solution. The experimental
178 surgery was performed by an experienced bioengineer and surgeon under the supervision of a senior
179 scientific officer at RBHSD, BARC, Mumbai, India. Apart from the usual oral surgical instruments,
180 innovative and delicate surgical instruments such as the aforementioned modified thin flexible blades,
181 specific to the experimental surgical protocol were used for extracting the tooth, atraumatically. Briefly,
182 the sterile modified blades were placed into the marginal gingiva of 301 in rabbits with the tip of the
183 blade proceeding apically whilst applying gentle finger pressure on the exterior of attached gingiva,
184 thereby guiding the blade in a careful and delicate oscillatory (forward and backward) linear motion
185 around the cervical^{3rd} of tooth circumference for tearing the gingival fibres. Later, an extended flexible
186 blade following closely the curvature of 301 in rabbits was gently inserted (towards the extremity i.e.
187 apically involving middle^{3rd} and apical^{3rd} of the tooth surface) under sterile saline-solution irrigation,

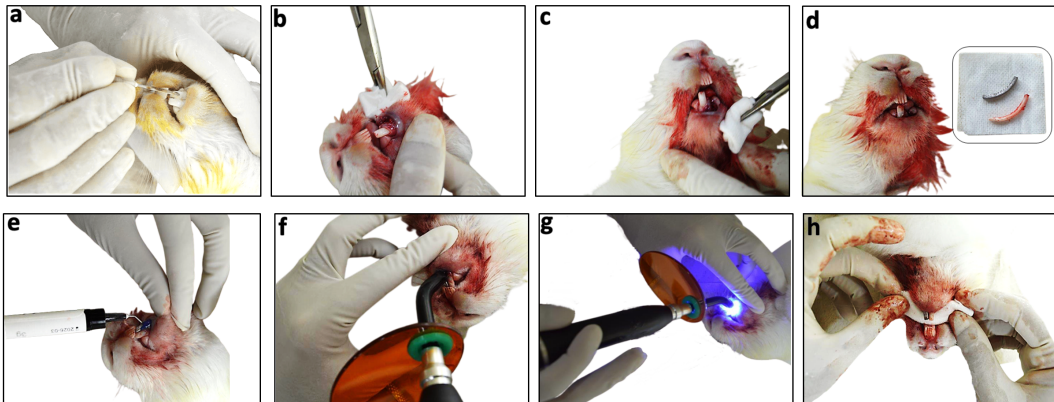


FIG. 2. Representative intraoperative photographs revealing the experimental surgical technique for installing titanium dental implant in the jaw of rabbit study models for achieving the desired functionality of “proprioception” in implants: (a) gentle insertion of the customized blade (flexible enough to follow the curvature of the entire root, preferably dimension of the blade should be smaller than that of the root) into the gingival sulcus and later continuing deep into the periodontal space with the tip of the blade angled towards the long axis of the tooth followed by cautious rocking motion around the entire tooth circumference for disengaging gingival and periodontal fibres respectively. The described surgical manoeuvre leads to severance of connective tissue attachment fibers bridging the tooth and alveolar bone and will render the tooth mobile and loose. Root fractures are avoided carefully. (b-c) inspection of the surgical site after grasping the tooth with the pediatric extraction forceps and applying gentle twisting / semi-rotatory motion along the transverse axis, together with the careful pulling of the tooth from the socket. (d) image of the oro-facial region of the rabbit study model after the extraction of mandibular left central incisor with an inset image showing a 3D-printed titanium dental implant i.e. the replacement model of the mandibular left central incisor and the actual extracted mandibular left central incisor tooth. Because coated test implant being white does not provide sharp coherent and intelligible information, an uncoated titanium implant was chosen for representing a good contrast in the intraoperative photographs. The primary stability of the implant is achieved by placing the sterile media wetted, push-fit implant carefully conforming its long axis to that in the entrance of the socket and later gently tapping it in the empty socket while stabilizing and supporting the jaw carefully. Dimensions of implant and tooth in all planes along with its curvature, coating thickness etc. needs to be accurately estimated to avoid complications like splitting of the socket during insertion of an implant which may further lead to complications/sequelae e.g. submental space infection in relation to mandibular anteriors etc.(e) after appreciative biomechanical stability of dental implant was achieved in the mandible of rabbit study models, a light-curing material based on methacrylate resin, was applied to protect the wound during the initial healing phase. The application area was 2 - 3.5 mm wide and approximately 1.5 - 1.8 mm thick. The material should adhere excellently and provide an impervious seal for both types of interfaces: peri-mucosal and endosseous interfaces so as to decrease the risk of surgical site infection, bleeding and negating the possibility of saliva contamination in the operative site. The application started covering the facial and lingual aspects of the bone-implant interface followed by using slight pressure proximally directed to the inter-dental space on either side.(f-g) the light-curing material was cured for 20 - 30 seconds using a polymerisation lamp, evenly in a scanning motion.(h) post-surgical inspection of the installed titanium implant, soft tissue and adjacent anatomical structures etc.

188 during which the tip of the index finger of the opposite hand was placed on the corresponding attached
189 gingiva to achieve stability and accurately placing the blade in the periodontal ligament space. The
190 blade within the periodontal space is gently twisted with minimal pressure and secured for 20-30 secs
191 for setting free the periodontal attachment fibres. Thereafter, the blade was further explored in the
192 periodontal space, moving all the way around the tooth with identical surgical manoeuvre. The loose
193 tooth, 301 is gently grasped by a pediatric extraction forceps and pulled out of the alveolar socket.

194 Proper installation of the customized endosseous dental implant after simple and clean surgical
195 extraction of 301 is the most crucial step. The primary stability of the implant (length = 2 mm shorter

196 than the total length of respective 301) is achieved by placing the push-fit implant carefully in the fresh
197 extraction socket and later gently tapping it with an orthopaedic mallet for its advancement in the entire
198 length of the fresh empty socket. Before placement, the implant is wetted with sterile culture media for
199 its easy gliding. The topmost, outer surface of the implant to be tapped should not be bevelled. Rather it
200 should be flat for even contact of mallet surface (during gentle tapping) resulting in proper distribution
201 of forces and uniform advancement of the implant along its long axis. Dimensions of implant and
202 respective tooth i.e. 301 along with its curvature is calculated with great precision (Supplementary
203 Fig) to avoid complications like splitting of the socket during insertion of implant etc. During the
204 push-fitting of implant the mandible of rabbit is stabilized and supported carefully. A light-curing resin
205 based barrier (PeroxiDam, Latus, Ukraine) was used to secure the interface of peri-implant soft tissue
206 and titanium implants from rest of the oral cavity. Additionally, rabbit no. 3 with test implant received
207 intramuscular 500 μ l q.d. of neurobion forte (Procter & Gamble Health Ltd. India) as a peripheral nerve
208 recovery agent. Post-operative pain control was achieved with subcutaneous administration of 0.05
209 mg kg⁻¹ buprenorphine hydrochloride. The rabbits were placed in individual cages during recovery.
210 Clinical assessment, detection of possible radiographic changes from routine postoperative radiographs,
211 physical examinations, monitoring etc. were included in the post-operative care and management. After
212 euthanasia, histopathological patterns of superficial cervical lymph nodes (Supplementary Fig), peri-
213 implant mucosa, tissue samples from spleen, liver, lung and kidney were evaluated. The relevant images
214 during surgery were recorded and captured by a Nikon B500 Camera.

215 **Results Of Experimental Surgery**

216 Essential findings of this proof-of-concept trial and its surgical outcome were performed at RBHSD,
217 BARC, (Mumbai, India) and provides conclusive evidence, indicating towards one of the advanced
218 possibility of biodegradable nanofibres coated implants. All surgeries were performed under general
219 anesthesia by an experienced bioengineer and surgeon. Immediate postoperative examination revealed
220 excellent primary stability for all implants (test and controls) placed in the mandible of all rabbit study
221 models. The post-operative assessment was carried out at the end of 24 and 48 hrs. Further examination
222 of the peri-implant site in the following days revealed normal and smooth tissue contour without any
223 evidence of discoloration, exudation, or crusting. All the rabbit study models were found to constantly
224 groom themselves. Subcutaneous administration of 0.05 mg kg⁻¹ buprenorphine hydrochloride for
225 all rabbits and 500 μ l q.d. of neurobion forte i.m. for rabbit no. 3 with test implants, additionally,
226 were continued. A sterile and soft diet with clean water was provided during the recovery period.
227 Assisted feeding was not attempted, as the rabbit(s) started eating by itself within 24-36 hrs, post-
228 surgery. It was observed that the rabbits were using the prehensile lips to assist in grasping softened
229 food, which was later masticated by the combined action of the tongue and posterior teeth. However,
230 at the beginning of the 8th day, upon close examination, the implants were noted to be displaced along
231 the longitudinal axis and were slightly shifted, mostly in a medial and posterior direction. Examination
232 of implants in the subsequent days confirmed various grades of mobility. Additionally, significant peri-
233 implant probing depth on mesial and distal aspects for both test and control implants were noted in
234 all rabbit study models when compared to that of a normal tooth. We found all implants had some
235 measurable grades of mobility at their respective interface; however, we do not have strong evidence to
236 suggest the specific and clear reason for such adverse effect on the bio-integration of test and control
237 implants in spite of such implants achieving initial firmness in bone with excellent primary stability
238 during surgery. Nevertheless, these findings suggest that implants of such dimensions are at risk of
239 exposure to some level of opposing occlusal forces thereby transferring and directing those to the

240 interface between the alveolar bone and implant. In all likelihood, the opposing structures mainly the
241 corresponding maxillary tooth occluding the dental implant resulted in undesirable changes in the peri-
242 implant bone level around the dental implant, leading to its loosening and subsequent dislodgement.
243 It is noted that, after immediate extraction, the selected dental implants replacing the tooth shouldn't
244 protrude more than 0.2 - 0.5 mm from the alveolar ridge to avert such occurrence. Following a thorough
245 evaluation and taking into account the extent of progressive bone loss and the effect of possible surgical
246 intervention with newer sets of implants (test and controls) with smaller dimensions replacing failed
247 ones at the exact surgical site, were planned. However, remnants of normal physiological and healthy
248 periodontal apparatus are necessary to accomplish the objectives successfully. Hence, a decision was
249 made to carry forward the research work with the exact surgical procedures described here, in another
250 set of animal study models with smaller dimensions of test and control implants.

251 Discussion

252 Restoration of malfunctioned or damaged peripheral nervous systems is an enormous challenge for the
253 therapeutic paradigms of stem cells. Osseointegrated dental implants are associated with the disruption
254 of proprioceptive pathways of teeth due to the missing PDL. Apart from the prosthodontic treatment
255 option serve by a dental implant, neural regeneration, and repair at its interface are additional research
256 objectives that have been taken in recently, towards the effective response, together as an "*advanced and*
257 *improved prosthetic remedy*" required for complete physiological recovery of the masticatory apparatus.

258 The present proof-of-concept trial deals with targeted repairing of the nerve terminals that are
259 present as an extension of the trigeminal system at the interface of the immediately placed dental
260 implant and alveolar bone, thereby completing the neural circuitry of a dental proprioceptive route
261 from the interface of a dental implant to the mesencephalic nucleus in the midbrain. Thus, in
262 addition to the endogenous stem cells in the peri-implant region, exogenous mesenchymal stem cells
263 seeded in the orthotopically placed nanofibrous coated implant in rabbit's mandible, was utilized for
264 neurogenesis/neural repair in peri-implant tissues so as to later gauge its proprioceptive features.

265 The results of our experimental surgery described herein include the actual extraction of the
266 complete tooth and installing an implant with minimal trauma to the adjacent structures. It is noted in the
267 trial that using force without proper detachment of fibres would most likely induce a transverse fracture
268 of the tooth at or below the gingival sulcus, making extraction with forceps impossible. Therefore,
269 the described surgical technique requires thorough training for the knowledge and understanding of
270 the related anatomical structures and implementation of the precise surgical skill, for executing the
271 installation strategies to induce proprioceptive features in dental implants.

272 The PCL/gelatine nanofibers, such as ours, supports the nerve cells and improve the neurite
273 outgrowth and cell differentiation process.⁵⁵ Additionally, it has been previously reported by us that the
274 titanium implants coated with PCL/gelatine nanofibrous scaffold, supports DPSCs, their proliferation
275 and subsequent neural differentiation.⁴² To ensure that the exogenous stem cells precisely participate
276 in the terminal nerve repair at the interface we have systemically administered *Neurobion Forte*, as a
277 peripheral nerve recovery agent^{56,57} in the rabbit study model with test implant.

278 However, additional specific interventional measures such as the inclusion of growth factors in
279 relation to peripheral nerve regeneration, such as Neurotrophin-3, Neurotrophin-4, Recombinant human
280 beta-NGF, and Fibroblast growth factors (FGF) protein⁵⁸ in the components of nanofibrous coating,
281 could have certainly resulted in further improvement in the overall objectives of the trial.

282 Further, in the process of bio-integration of such nanofibrous coated implants, the coating will
283 gradually deteriorate⁵⁹ resulting in shifting of the implant-bone interface medially in relation to

284 longitudinal axis of the dental implant. As the implantation period progresses, we assume that
285 the available degradation site will most probably be occupied by tissues having features similar to
286 periodontium, progressively repairing terminal nerve endings with anastomosis and finally bridging
287 alveolar bone and implant surface.

288 Histological staining often permits initial recognition of the cellular and structural features of
289 the regenerated tissue approximating the implant surfaces. The peculiarities of the repaired neural
290 framework, secured in the confined periprosthetic tissue could be analysed by histological methods
291 confirming morphological changes after nerve regeneration. Injuries such as those induced by exodontia
292 may damage a significant population of the peripheral axons of sensory bipolar neurons innervating the
293 teeth,⁶⁰ initiating the mechanism of axonal regeneration at the injury site.⁶¹ Later, a high number of
294 regenerating clusters with Schwann cells elaborate processes⁶² could be identified in the recovering
295 region.

296 The restored trigeminal proprioceptive pathway together with its specialized sensory discriminative
297 features could further be corroborated in preclinical animal models using electroencephalographic,
298 magnetoencephalographic⁶³ and fMRI approaches⁶⁴ etc. (Supplementary Fig).

299 Contributions

300 S.D. and J.B. designed the research plan, S.D. performed the experiments, surgery and other tasks
301 related to the project, wrote the manuscript and made the figures. Results were reviewed by J.B, H.D.S.
302 and S.D and modifications jointly done. S.D was jointly supervised by H.D.S. and J.B.

303 Acknowledgments

304 The authors gratefully acknowledge IIT Bombay and BARC, Mumbai for access to Central and
305 Departmental facilities for this largely self-funded work. The authors also wish to express their sincere
306 thanks to BETiC facility for the 3D-printing of titanium implants.

307 Funding

308 The work was jointly supported by IIT Bombay (*J.B. personal research funds*) and BARC, Mumbai,
309 India.

310 References

- 311 1. Liang, Y., Luan, X. Liu, X. Recent advances in periodontal regeneration: A biomaterial perspective.
312 *Bioact. Mater.* 5, 297–308 (2020).
- 313 2. Haggard, P. de Boer, L. Oral somatosensory awareness. *Neurosci. Biobehav. Rev.* 47, 469–484
314 (2014).
- 315 3. Rodella, L. F., Buffoli, B., Labanca, M. Rezzani, R. A review of the mandibular and maxillary
316 nerve supplies and their clinical relevance. *Arch. Oral Biol.* 57, 323–334 (2012).
- 317 4. van Steenberghe, D. The structure and function of periodontal innervation: A review of the
318 literature. *J. Periodontal Res.* 14, 185–203 (1979).
- 319 5. Misch, C. E. *Dental implant prosthetics-E-book.* (Elsevier Health Sciences, 2004).
- 320 6. Branemark, P.-I. Osseointegrated implants in the treatment of the edentulous jaw. Experience from
321 a 10-year period. *Scand J Plast Reconstr Surg Suppl* 16, (1977).

- 322 7. Branemark, P.-I. Osseointegration and its experimental background. *J Prosthet Dent* 50, 399–410
323 (1983).
- 324 8. Lee, D.-J. et al. Bio-implant as a novel restoration for tooth loss. *Sci. Rep.* 7, 1–10 (2017).
- 325 9. Higaki, N. et al. Do sensation differences exist between dental implants and natural teeth?: a meta-
326 analysis. *Clin. Oral Implants Res.* 25, 1307–1310 (2014).
- 327 10. Klineberg, I. Murray, G. Osseoperception: sensory function and proprioception. *Adv. Dent. Res.*
328 13, 120–129 (1999).
- 329 11. Williams, W. N., Levin, A. C., LaPointe, L. L. Cornell, C. E. Bite force discrimination by
330 individuals with complete dentures. *J. Prosthet. Dent.* 54, 146–150 (1985).
- 331 12. Oshima, M. et al. Functional tooth restoration by next-generation bio-hybrid implant as a bio-hybrid
332 artificial organ replacement therapy. *Sci. Rep.* 4, 1–10 (2014).
- 333 13. Marei, M. K., Saad, M. M., El-Ashwah, A. M., El-Backly, R. M. Al-Khodary, M. A. Experimental
334 formation of periodontal structure around titanium implants utilizing bone marrow mesenchymal
335 stem cells: a pilot study. *J. Oral Implantol.* 35, 106–129 (2009).
- 336 14. Parlar, A. et al. New formation of periodontal tissues around titanium implants in a novel dentin
337 chamber model. *Clin. Oral Implants Res.* 16, 259–267 (2005).
- 338 15. Choi, B.-H. Periodontal ligament formation around titanium implants using cultured periodontal
339 ligament cells: a pilot study. *Int. J. Oral Maxillofac. Implants* 15, (2000).
- 340 16. Jahangiri, L., Hessamfar, R. Ricci, J. L. Partial generation of periodontal ligament on endosseous
341 dental implants in dogs. *Clin. Oral Implants Res.* 16, 396–401 (2005).
- 342 17. Gault, P. et al. Tissue-engineered ligament: implant constructs for tooth replacement. *J. Clin.*
343 *Periodontol.* 37, 750–758 (2010).
- 344 18. Lin, Y. et al. Bioengineered periodontal tissue formed on titanium dental implants. *J. Dent. Res.* 90,
345 251–256 (2011).
- 346 19. da Silva, J. M. et al. An Active Implant to Restore Dental Proprioceptivity. in 2020 23rd Euromicro
347 Conference on Digital System Design (DSD) 316–319 (IEEE, 2020).
- 348 20. Xu, X. et al. Biodegradable engineered fiber scaffolds fabricated by electrospinning for periodontal
349 tissue regeneration. *J. Biomater. Appl.* 36, 55–75 (2021).
- 350 21. Wu, T., Mo, X. Xia, Y. Moving Electrospun Nanofibers and Bioprinted Scaffolds toward
351 Translational Applications. *Adv. Healthc. Mater.* 9, 1901761 (2020).
- 352 22. Peng, W. et al. MgO Nanoparticles-Incorporated PCL/Gelatin-Derived Coaxial Electrospinning
353 Nanocellulose Membranes for Periodontal Tissue Regeneration. *Front. Bioeng. Biotechnol.* 9,
354 668428 (2021).
- 355 23. Rao, F. et al. Aligned chitosan nanofiber hydrogel grafted with peptides mimicking bioactive brain-
356 derived neurotrophic factor and vascular endothelial growth factor repair long-distance sciatic nerve
357 defects in rats. *Theranostics* 10, 1590–1603 (2020).
- 358 24. Linden, R. W. An update on the innervation of the periodontal ligament. *Eur. J. Orthod.* 12, 91–100
359 (1990).
- 360 25. Barral, J.-P. Croibier, A. Maxillary nerve. in *Manual Therapy for the Cranial Nerves* 129–138
361 (Elsevier, 2009).doi:10.1016/B978-0-7020-3100-7.50019-7.
- 362 26. Barral, J.-P. Croibier, A. Mandibular nerve. in *Manual Therapy for the Cranial Nerves* 139–146
363 (Elsevier, 2009). doi:10.1016/B978-0-7020-3100-7.50020-3.
- 364 27. Frisdal, A. Trainor, P. A. Development and evolution of the pharyngeal apparatus. *Wiley*
365 *Interdiscip. Rev. Dev. Biol.* 3, 403–418 (2014).
- 366 28. Razek, A. A. Huang, B. Y. Lesions of the petrous apex: classification and findings at CT and MR
367 imaging. *Radiographics* 32, 151–173 (2012).

- 368 29. Henssen, D. J. et al. New insights in trigeminal anatomy: a double orofacial tract for nociceptive
369 input. *Front. Neuroanat.* 10, 53 (2016).
- 370 30. Woolfall, P. Coulthard, A. Trigeminal nerve: anatomy and pathology. *Br. J. Radiol.* 74, 458–467
371 (2001).
- 372 31. Wang, C.-Z. et al. Development of the mesencephalic trigeminal nucleus requires a paired
373 homeodomain transcription factor, Drg11. *Mol. Cell. Neurosci.* 35, 368–376 (2007).
- 374 32. Bradnam, L. Barry, C. The role of the trigeminal sensory nuclear complex in the pathophysiology
375 of craniocervical dystonia. *J. Neurosci.* 33, 18358–18367 (2013).
- 376 33. Tal, M. Devor, M. Anatomy and neurophysiology of orofacial pain. *Orofac. Pain Headache Edinb.*
377 Elsevier 19–44 (2008). 34. Kritzer, M. *A Textbook of Neuroanatomy.* (2007).
- 378 34. Kritzer, M. *A Textbook of Neuroanatomy.* (2007).
- 379 35. Hendry, S. H. Hsiao, S. S. Fundamentals of sensory systems. in *Fundamental Neuroscience: Fourth*
380 *Edition* 499–511 (Elsevier Inc., 2013).
- 381 36. Fillmore, E. P. Seifert, M. F. Anatomy of the trigeminal nerve. *Nerves Nerve Inj.* 319–350 (2015).
- 382 37. D’Antoni*, A. V. *Gray’s Anatomy, the Anatomical Basis of Clinical Practice, Forty-First Edition,*
383 *by Susan Standring, Editor-in-Chief, Elsevier Limited, 2016, 1,562 Pages, Hardcover, 228.99(*
384 *171.74), ISBN: 978-0-7020-5230-9.* (2016).
- 385 38. Michael-Titus, A., Revest, P. Shortland, P. The Spinal Cord. in *The Nervous System* 59–78
386 (Elsevier, 2010). doi:10.1016/B978-0-7020-3373-5.00004-6.
- 387 39. Das, S. et al. Accentuated osseointegration in osteogenic nanofibrous coated titanium implants. *Sci.*
388 *Rep.* 9, 17638 (2019).
- 389 40. Das, S. et al. Osteogenic Nanofibrous Coated Titanium Implant Results in Enhanced
390 Osseointegration: In Vivo Preliminary Study in a Rabbit Model. *Tissue Eng. Regen. Med.* 15,
391 231–247 (2018).
- 392 41. Das, S., Soni, V. P. Bellare, J. R. Tissue Engineering Strategies for Tooth and Dento-alveolar Region
393 with Engineered Biomaterial and Stem Cells. in *Biointerface Engineering: Prospects in Medical*
394 *Diagnostics and Drug Delivery* (eds. Chandra, P. Pandey, L. M.) 31–54 (Springer Singapore, 2020).
395 doi:10.1007/978-981-15-4790-4_2.
- 396 42. Das, S. Bellare, J. R. Dental Pulp Stem Cells in Customized 3D Nanofibrous Scaffolds for
397 Regeneration of Peripheral Nervous System. in *Stem Cell Nanotechnology* (ed. Turksen, K.) vol.
398 2125 157–166 (Springer US, 2018).
- 399 43. Osofsky, A., LeCouteur, R. A. Vernau, K. M. Functional neuroanatomy of the domestic rabbit
400 (*Oryctolagus cuniculus*). *Veterinary Clin. North Am. Exot. Anim. Pract.* 10, 713–730 (2007).
- 401 44. Chai, Y., Chen, M., Zhang, W. Zhang, W. Somatotopic organization of trigeminal ganglion: three-
402 dimensional reconstruction of three divisions. *J. Craniofac. Surg.* 25, 1882–1884 (2014).
- 403 45. Herta, J. et al. An experimental animal model for percutaneous procedures used in trigeminal
404 neuralgia. *Acta Neurochir. (Wien)* 159, 1341–1348 (2017).
- 405 46. Meessen, H. Olszewski, J. A cytoarchitectonic atlas of the rhombencephalon of the rabbit.
406 *Cytoarchitectonic Atlas Rhombencephalon Rabbit* (1949).
- 407 47. Capra, N. F. Desseu, D. Central connections of trigeminal primary afferent neurons: topographical
408 and functional considerations. *Crit. Rev. Oral Biol. Med.* 4, 1–52 (1992).
- 409 48. Standard, I. S. O. 10993-6. Biological evaluation of medical devices–Part 6: Tests for local effects
410 after implantation. Geneva Switz. *Int. Organ. Stand.* (2007).
- 411 49. Control, C. for the P. of Animals, S. on E. on. CPCSEA Guidelines for laboratory animal facility.
412 *Indian J Pharmacol* 35, (2003).
- 413 50. Baxter, C. J. Veterinary dentistry: a clinician’s viewpoint. *Dent. Update* 40, 386–390 (2013).

- 414 51. Floyd, M. R. The modified Triadan system: nomenclature for veterinary dentistry. *J. Vet. Dent.* 8,
415 18–19 (1991).
- 416 52. Lee, J. et al. The impact of surface treatment in 3-dimensional printed implants for early
417 osseointegration: a comparison study of three different surfaces. *Sci. Rep.* 11, 1–10 (2021).
- 418 53. Bowman, M. Sharpening common workshop tools. (2020).
- 419 54. Fragiskos, F. D. Oral surgery. (Springer Science Business Media, 2007).
- 420 55. Ghasemi-Mobarakeh, L., Prabhakaran, M. P., Morshed, M., Nasr-Esfahani, M.-H. Ramakrishna,
421 S. Electrospun poly(-caprolactone)/gelatin nanofibrous scaffolds for nerve tissue engineering.
422 *Biomaterials* 29, 4532–4539 (2008).
- 423 56. Baltrusch, S. The Role of Neurotropic B Vitamins in Nerve Regeneration. *BioMed Res. Int.* 2021,
424 1–9 (2021).
- 425 57. Altun, I. Kurutaş, E. B. Vitamin B complex and vitamin B12 levels after peripheral nerve injury.
426 *Neural Regen. Res.* 11, 842 (2016).
- 427 58. McMahan, S. B. Priestley, J. V. Peripheral neuropathies and neurotrophic factors: animal models
428 and clinical perspectives. *Curr. Opin. Neurobiol.* 5, 616–624 (1995).
- 429 59. Dong, Y., Liao, S., Ngiam, M., Chan, C. K. Ramakrishna, S. Degradation behaviors of electrospun
430 resorbable polyester nanofibers. *Tissue Eng. Part B Rev.* 15, 333–351 (2009).
- 431 60. Byers, M. R. Dental sensory receptors. *Int. Rev. Neurobiol.* 25, 39–94 (1984).
- 432 61. Campbell, W. W. Evaluation and management of peripheral nerve injury. *Clin. Neurophysiol.* 119,
433 1951–1965 (2008).
- 434 62. Geuna, S. et al. Chapter 3 Histology of the Peripheral Nerve and Changes Occurring During Nerve
435 Regeneration. in *International Review of Neurobiology* vol. 87 27–46 (Elsevier, 2009).
- 436 63. Hihara, H. et al. Somatosensory evoked magnetic fields of periodontal mechanoreceptors. *Heliyon*
437 6, e03244 (2020).
- 438 64. Trulsson, M., Francis, S. T., Bowtell, R. McGlone, F. Brain Activations in Response to Vibrotactile
439 Tooth Stimulation: a Psychophysical and fMRI Study. *J. Neurophysiol.* 104, 2257–2265 (2010).

